Review article

Molecular modelling and simulation in fluid process engineering

Martin Horsch* **and Hans Hasse**

University of Kaiserslautern, Laboratory of Engineering Thermodynamics, Erwin-Schrödinger-Str. 44, 67663 Kaiserslautern, Germany

Molecular simulation has reached a high degree of versatility due to the advance of massively-parallel high performance computing. On the basis of physically realistic models of the intermolecular interactions, thermodynamic properties can be described and predicted with a high accuracy. Transport processes and heterogeneous systems can today be reliably simulated as well. This requires robust molecular models and simulation methods with a rigorous foundation on statistical mechanics. The state of the art is discussed here with a focus on applications in process engineering.

Keywords: Molecular simulation, interfaces, transport processes, high performance computing

1. INTRODUCTION

Following the development of Monte Carlo (MC) simulation methods at Los Alamos in the 1950s, molecular simulation rapidly gained recognition as a numerical approach for computing thermodynamic properties on the foundation of statistical mechanics [1 – 3]. Molecular simulation is therefore one of the first applications of scientific computing. While MC simulation is randomized and generates statistics over representative molecular configurations, molecular dynamics (MD) follows the temporal evolution of the simulated systems [2]. The early success of molecular approaches in scientific computing is due to the fact that relatively few molecules (about 200 to 1 000) are sufficient to reproduce most thermodynamic properties of homogeneous fluids. This also applies to phase equilibria, and particularly vapour-liquid equilibria (VLE), which can be investigated by simulating the coexisting homogeneous phases separately, e.g. with the Grand Equilibrium method [4], without considering the phase boundary explicitly.

The basis for a molecular simulation is the molecular model, i.e. a numerically favourable representation of the interactions between the molecules as a classical-mechanical force field. Even very simple models, such as hard spheres, are sufficient to reproduce many physical phenomena qualitatively and to investigate the underlying mechanisms at the molecular level. In most cases, the parameters of a model that is qualitatively correct can be optimized to reach a good quantitative agreement with real fluid properties [5 – 8]. The remarkable progress of simulation technology in high performance computing, concerning both the hardware and the simulation methods, has led to the emergence of Computational Molecular Engineering as an independent discipline of mathematical modelling and simulation that now delivers a significant contribution to scientific research in fluid process engineering [3, 7 – 9].

Beside MC and MD simulation, there are various further numerical methods in molecular thermodynamics which all have their respective weaknesses and strengths [8]. This includes mesoscopic approaches, such as Lattice Boltzmann simulation or classical-mechanical density functional theory, which occupy an intermediate position between molecular and continuum mechanics [10]. Such methods can

*Corresponding author: Martin Horsch, martin.horsch@mv.uni-kl.de, phone: +49 631 205 3227, fax: +49 631 205 3835.

bridge greater length and time scales, which often, however, goes at the expense of quantitative reliability. Moreover, molecular equations of state on the basis of the statistical associating fluid theory have a great potential for correlating and predicting real fluid properties [5, 8, 10, 11]. There is a strong and fruitful tendency within Computational Molecular Engineering to combine several approaches, e.g. by conducting coupled scale-bridging simulations [12] or by employing a consistent force field for molecular simulations and equations of state [5].

The simulation of technical processes at surfaces, such as sputtering [13], may require reliable multibody potentials for the interaction between atoms in the solid phase. Such models can be highly complex and have a large number of adjustable parameters [14]. Similarly, the conformation of macromolecules with a large number of internal degrees of freedom is in principle accessible to molecular simulation. However, the parameterization of the force field for macromolecules constitutes a major challenge, and the exploration of the free-energy landscape for relatively slow conformation transitions, such as protein folding, requires elaborate sampling techniques [15]. In fundamental research in physics, where molecular methods have their origin, simulations with abstract qualitative models can still yield fruitful insights. For instance, the simulation of hard spheres contributes to understanding the molecular structure of liquids [16].

The state of the art in molecular modelling and simulation is commented here with regard to possible applications in fluid process engineering. In thermodynamics, molecular methods have an inherent advantage over empirical correlations of the available data. By selecting a physical model which explicitly accounts for microscopic properties and intermolecular interactions, the choice of adequate model parameters facilitates at least the same level of numerical agreement with real fluid properties as phenomenological approaches. In many cases, on the basis of both molecular equations of state and molecular simulation, Computational Molecular Engineering reaches a greater accuracy than the underlying experimental data, which then become the main source of error [5, 8].

2. COMPUTATIONAL MOLECULAR ENGINEERING

2.1 Molecular modelling of fluids

Quantitative agreement with thermodynamic properties of real fluids is decisive for the applicability of a model in an engineering framework. Reliability for the extrapolation and prediction of properties is equally important in many cases. On the basis of a physically realistic description, with a small number of adjustable parameters, these objectives can both be reached. Accordingly, molecular force field methods are based on a classical-mechanical model of the forces acting between molecules. These forces are determined from pair potentials $u(r)$ which contribute to the potential energy of the system and are defined in terms of the distance r between pointwise interaction sites that belong to different molecules. The Lennard-Jones (LJ) potential

$$u(r) = 4\varepsilon \left[(\sigma / r)^{12} - (\sigma / r)^{6}\right],$$

with the parameters ε (energy) and σ (size), reproduces short-range interactions between molecules in a numerically effective way, accounting for attraction by dispersive London forces and for soft repulsion due to the interpenetration of non-bonding molecule orbitals [2, 6]. Long-range electrostatic interactions can be represented by point charges and a multipole expansion in terms of higher-order point polarities.

The combination of a single LJ interaction site with a point charge, e.g., yields a suitable model for alkali and halide ions [17]. Adequately arranging two point charges in combination with a LJ site accounts for polarity as well as hydrogen bonding, so that the structure and dynamics of hydrogen bonds as well as the influence of intermolecular association on the thermodynamic properties can be reproduced [18], cf.

Fig. 1. For this purpose, it is crucial to consider the geometric asymmetry of the hydrogen bond. If this asymmetry is neglected and the LJ site is placed in the middle between the two point charges, cf. Fig. 1 (bottom), the VLE and the critical temperature are exclusively controlled by the LJ parameters and the dipole moment. With this unphysical arrangement, therefore, the distance between the point charges, which controls hydrogen bonding, does not have a significant influence on the thermodynamic properties of the model. If the point charges are arranged asymmetrically, however, a distinct influence of hydrogen bonding can be isolated from that of the dipole, cf. Fig. 1 (top). In this case, at constant dipole strength, a greater distance between the point charges induces a greater orientation-dependent attraction due to hydrogen-bonded association [18].

Modelling approaches which have a sound physical background can reach a high degree of agreement with real material properties if they possess free parameters that can be adjusted. Homogeneous fluid properties, including linear transport coefficients [19, 20], can then be reproduced, cf. Fig. 2. Furthermore, VLE data and interfacial tensions are modelled consistently [21], cf. Fig. 3. Even the single-centre LJ potential, which has two parameters, is an adequate model for noble gases and for methane [2, 6]. The LJTS model, where the LJ potential is truncated at $r = 2.5\,\sigma$, can also be employed for simulating these fluids. Molecular models with two equal LJ sites and one point dipole (2CLJD) or one point quadrupole (2CLJQ), respectively, have four parameters and are sufficient to reliably represent most low-molecular fluids. If the exponents for the repulsive and attractive contributions to the pair potential are also included among the model parameters, the Mie potential is obtained as a generalization of the LJ model. The Mie potential can be fruitfully used as a coarse-grained model, e.g. representing CO_2 accurately with a single interaction site and even relatively complex molecules with only a few interaction sites [5].

In all cases, it is decisive to optimize the quantitative accuracy of the model by parameterizing it accordingly. Usually, it is sufficient to minimize a single objective function such as the mean square deviation from a correlation of experimental VLE data [7]. Alternatively, the entire set of Pareto-optimal parameter combinations can be computed for multicriteria optimization. This facilitates a flexible modelling approach that permits a free choice of suitable parameter values depending on the considered scenario [6, 21]. For complex models with a large number of interaction sites it is generally beneficial to follow an approach that integrates simulations and equations of state or correlations of model properties. In this way, the numerical efficiency of model parameterization can be increased [5].

Molecular models can be validated empirically by testing their ability to extrapolate thermodynamic properties [3]. This typically means to compare the results of molecular simulations with additional experimental data that were not considered for the parameterization [7]. These simulations are predictions on the basis of the molecular model, and the quality of the prediction reflects the quality of the model. Beside quantitative extrapolation, where the thermodynamic boundary conditions are varied, the predictive capacity for qualitatively different properties can be assessed. For example, a good agreement with the experimentally measured surface tension can be obtained even for models which were only adjusted to VLE data from simulations of homogeneous systems [6, 21], cf. Fig. 3. For mixtures, a pair potential acting between unlike molecules also needs to be specified. In case of electrostatic interaction sites, i.e. point charges and point polarities, the unlike interaction follows Coulomb's law, and no binary interaction parameters are present. For the LJ potential, empirical combination rules – such as the Lorentz-Berthelot rule – can be used, employing binary interaction parameters if required [22].

2.2 Molecular simulation in high performance computing

Beside a sound modelling approach, a numerically efficient evaluation and parameterization of the model is a prerequisite for its viability as a practical engineering tool. Computational Molecular Engineering, just as other comparable methods such as computational fluid dynamics, is a major application area for high performance computing. During model optimization, for instance, many different parameter sets need to

be considered and assessed with regard to their agreement with real fluid properties such as VLE data. Thereby, each parameter combination that is evaluated requires a series of VLE simulations, each of which needs to reach engineering-level precision.

The efficient parallel execution of numerous simulation runs for relatively small homogeneous systems can be implemented by parallelizing the computation of pair potentials and forces. This approach, which is e.g. implemented in the simulation code *ms2* [9], requires a communication of the positions and velocities of all particles between all parallel processes after each MC or MD step. For simulations of large systems, this becomes inefficient in comparison to a volume-based domain decomposition scheme, cf. Fig. 4, where only processes that simulate immediately adjacent subdomains need to exchange the coordinates of particles within a relatively small boundary region. In this way, a system containing four trillion molecules was successfully considered by molecular simulation using the MD code *ls1 mardyn* on the SuperMUC cluster at the Leibniz Computing Centre [23].

Furthermore, with large numbers of molecules, it becomes impracticable to compute intermolecular distances and pair potentials for all pairs of molecules explicitly. Instead, the molecules are sorted spatially by neighbour lists or a linked-cell data structure. Using adaptive cells and a dynamic load balancing strategy for parallel execution, cf. Fig. 4, even systems with highly heterogeneous or fluctuating molecule distributions can be simulated efficiently. For instance, this can be accomplished by a data structure based on *k*-dimensional trees (k-d trees) which recursively bisect the simulation volume into subdomains such that each of the parallel processes carries approximately the same computational load. The innermost loops of the code then only need to be executed for the relatively limited number of molecule pairs from a single cell or two immediately adjacent cells [23].

As Fig. 5 shows for the case of the MD simulation of a droplet with 3.7 million molecules, load balancing by k-d trees with an adaptive linked-cell data structure significantly improves the scalability of the code. In this way, supercomputers with a large number of cores can be used efficiently. By massively-parallel high performance computing, molecular simulation becomes an experiment *in silico*. It follows processes in systems with heterogeneous density distributions, such as flow through nano- and microporous membranes [24 – 26], and can contribute to understanding complex activated processes such as nucleation in supersaturated vapours [27].

3. APPLICATIONS IN FLUID PROCESS ENGINEERING

3.1 Thermodynamic properties

A broad range of thermodynamic properties of fluids is immediately accessible to molecular modelling and simulation. Beside quantities such as the density, pressure, temperature, and composition of homogeneous fluid phases, this includes phase coexistence behaviour, such as VLE, LLE, and other multiphase systems. Even large gaps in experimental data bases can be bridged by molecular simulation, since it is possible to adjust the molecular models to a small number of experimental data points. For systems including hazardous compounds and for thermodynamic boundary conditions that are hard to impose experimentally, this can significantly reduce the cost of measuring these properties in the laboratory. This potential has been known to the chemical industry for some time, e.g. from the response of the molecular simulation community to the challenge problems posed by the Industrial Fluid Properties Simulation Collective.

However, molecular modelling and simulation can be far more than a tool for predicting homogeneous fluid properties in equilibrium. Various complex application scenarios with a particular importance for process engineering can illustrate this: Based on the accurate reproduction of structure and dynamics on the nanometre and nanosecond scales, molecular simulation is highly suitable for investigating interfacial

properties (Section 3.2) and transport processes (Section 3.3). For processes at phase boundaries, such as droplet dynamics or nucleation, molecular methods are particularly powerful when they are combined with high performance computing [23, 27].

3.2 Properties of fluids at interfaces

By resolving the molecular structure of the fluid at a phase boundary, it becomes possible to investigate interfacial phenomena in detail. In molecular simulations, e.g., the continuous transition between two fluid phases and the layer structure imposed on fluid matter adsorbed at a solid surface become visible, cf. Fig. 6. In addition to the average density distribution, fluctuations and waves at the interface are computed, so that even configurations far from mechanical equilibrium are accurately taken into account. It becomes possible to investigate the mechanisms on the molecular level which underlie quantities that are accessible to phenomenological thermodynamics only in terms of effective excess properties of the interface. For instance, the adsorption Γ_i, i.e. the excess density of a component at an interface, and the surface tension γ, i.e. the interfacial excess free energy, are directly accessible by molecular simulation of heterogeneous systems. The Gibbs adsorption equation

$$\left(\frac{\partial \gamma}{\partial \mu_i}\right)_{T,\mu_{j\neq i}} = -\Gamma_i$$

relates these quantities to the chemical potential μ_i, which can also be obtained from the simulations. As shown in Fig. 7, there can be a significant enrichment of one of the components at the interface even for mixtures of low-molecular fluids. Experimentally, this effect can only be observed indirectly, by measuring the dependence of the surface tension on the composition of the mixture.

At planar fluid interfaces, mechanical and thermodynamic approaches for defining and computing the surface tension yield the same result, so that the surface tension can be computed immediately from the pressure tensor of the simulated system [1, 28]. This method can be straightforwardly combined with cut-off corrections for heterogeneous systems which separate short-range and long-range interactions efficiently [21]. At curved interfaces, an integral over the mechanical pressure tensor does not yield the thermodynamic surface tension rigorously, and a contribution of the second-order virial needs to be taken into account [28].

A particular challenge for molecular methods consists in reaching quantitative reliability for modelling adsorption. Beside the force field for the fluid, this also requires a representation of the solid phase and the interaction between fluid molecules and the adsorber surface [29]. Moreover, the substrate can possess regular and irregular structures that combine to form a complex morphology [30]. Due to their heterogeneous structure, systems with a phase boundary have stronger long-range interactions which also need to be taken into account [21]. Developments in this direction are promising, and they profit from various advantages of molecular simulation over purely empirical methods. On the basis of validated molecular models, multiple adsorbed layers can be predicted without resorting to overly simplified approximations from phenomenological thermodynamics [1, 30].

Wetting of a solid by a fluid can be considered by simulating the three-phase contact between a vapour-liquid interface and the surface of a solid substrate. Fig. 6 shows a density profile from the simulation of a droplet on a planar wall, both modelled by the LJTS potential [29]. Multiple ordered adsorbed layers from the liquid phase and a single adsorbed layer from the gas phase can be discerned. This linear order interferes in a non-trivial way with the approximately spherical shape of the droplet and yields a molecular structure that cannot be uncovered experimentally and can hence only be revealed by molecular simulation. Contact angles from the simulation can be compared to experimental data to parameterize the fluid-wall interaction [29, 30], assuming that the structure of the experimentally considered system is

realistically modelled, accounting for surface roughness, irregularities, and other imperfections of the surface, such as residual adsorbed matter.

3.3 Transport processes and non-equilibria

Transport properties such as thermal conductivities, viscosities, and diffusion coefficients are experimentally accessible and highly relevant for numerous applications in process engineering. In heterogeneous systems, however, e.g. at a wall or close to a phase boundary, the dissipation occurring by heat, momentum, and mass transfer is often non-linear or characterized by complex boundary conditions [31], which have to be understood to accurately describe mass transfer through nanoporous materials [24 – 26]. Activated processes are often empirically modelled by approaches based on Arrhenius equations which reduce a possibly complex transition process to the magnitude of a single free energy barrier. Here, molecular simulation can help to gain a deeper understanding [27, 32, 33].

For the computation of transport properties, a fluid is analysed either by equilibrium MD (EMD), which applies relations from statistical mechanics [20], or a non-equilibrium state is simulated by non-equilibrium MD (NEMD) to observe the relaxation process which is caused by the deviation from equilibrium [25]. Many such processes follow a law of linear response, as long as this deviation is relatively small, and can then be described by linear transport coefficients. Statistical mechanics rigorously relates these properties, which characterize the dissipation occurring in a non-equilibrium state, with the fluctuation of corresponding quantities in the equilibrium state.

By evaluating the Einstein relation, e.g., the self-diffusion coefficient is obtained immediately from the mean square displacement of single molecules over time. With the Green-Kubo formalism, transport properties can be determined from integrals over autocorrelation expressions $\omega(0) \cdot \omega(t)$ for characteristic observables ω. Small systems (with about 1 000 molecules) are suitable for EMD methods. However, the memory requirements for computing the autocorrelation are substantial, and long simulations are needed to obtain robust statistics. In Fig. 2, EMD simulation results are shown for binary mixtures of methanol and ammonia. The molecular models were adjusted to quantum-mechanical computations and experimental VLE data. A good agreement between model predictions and real fluid properties is obtained here as well [20].

Transport phenomena can also be investigated directly by MD simulation. Starting from an unstable initial state, the relaxation process can be followed until the equilibrium is reached. Beside the transport properties, such direct simulations of relaxation can also yield further insights on the respective processes. In NEMD simulation, a stationary non-equilibrium state is simulated instead. In this way, the velocity of the relaxation process and the transport coefficient can be obtained at a high accuracy under constant and well-defined boundary conditions. Such methods require the intervention of a Maxwellian daemon, e.g. in form of a driving force, which upholds the non-equilibrium state.

This approach has numerous applications for the simulation of micro- and nanofluidics [24], e.g. flow through nanoporous membranes [25, 26]. Collective diffusion coefficients of fluids in contact with a nanostructured solid substrate can be computed by NEMD with Avendaño's daemon [25], which acts on a part of simulation volume to accelerate differently labelled, but otherwise identical molecules in opposite directions. Analogous simulation methods can capture the local shear viscosity of the fluid and the pressure drop in a nanofluidics scenario. Thereby, molecular simulation can reproduce entrance and exit effects, cf. Fig. 8, which can be particularly relevant for filtration. The main advantage of NEMD over EMD is that it also applies to transport processes in the non-linear regime, e.g. for non-Newtonian fluids or extreme driving forces.

Due to its molecular resolution, MD simulation is particularly suitable for investigating coupled heat and

mass transfer during a phase transition such as vaporization by pool boiling or condensation in a supersaturated vapour. These processes are activated, starting from a metastable state, and are initialized by the formation of dispersed nanoscopic nuclei of the phase that is thermodynamically stable under the respective conditions. The first step of the process is nucleation, by which supercritical nuclei emerge after a free energy barrier has been overcome. Even though nucleation, as an activated process, is more complex than spontaneous relaxation processes, it can also be simulated directly. In this case, a single MD simulation can reproduce the whole phase transition. A related NEMD approach consists in simulating the pseudo-grand canonical ensemble with McDonald's daemon: This Maxwellian daemon removes large nuclei of the emerging dispersed phase, and the nucleation rate can be determined from the frequency of these interventions [27].

4. CONCLUSION

Molecular modelling is a reliable method for describing and predicting thermodynamic properties. Moreover, massively-parallel MD simulation of large heterogeneous systems can contribute to elucidating the molecular effects that underlie transport processes at interfaces. Reaching quantitative agreement with real fluid properties, this constitutes a promising approach for optimizing engineering processes, in particular, if solid surfaces and their contact with the fluid are represented realistically.

The knowledge of phase equilibrium data, in combination with wetting properties, is of interest for many applications in process engineering such as distillation. Adsorption isotherms as well as adsorption and desorption kinetics can be simulated directly. Furthermore, it suggests itself to explore applications in extraction and the design of cyclic processes. Only part of the way from basic research to systematic applications in process optimization has been gone for molecular methods so far. However, it can already be recognized that it will pay off to go the remaining steps.

Acknowledgment. We would like to thank S. Becker, W. Eckhardt, C. Engin, S. Grottel, G. Guevara Carrión, C. Niethammer, G. Reina, and S. Werth for their contributions to simulation and visualization, C. Avendaño Jiménez, S. V. Lishchuk, E. A. Müller, F. Siperstein, R. Srivastava, N. Tchipev, and J. Vrabec for fruitful discussions, the German Federal Ministry of Education and Research (BMBF) for funding the SkaSim project, and the German Research Foundation (DFG) for funding the Collaborative Research Centre (SFB) 926 and the Reinhart Koselleck project of one of the authors (H.H.). The present work was conducted under the auspices of the Boltzmann-Zuse Society for Computational Molecular Engineering (BZS).

LITERATURE

[1] J. S. Rowlinson, B. Widom, *Molecular Theory of Capillarity*, Clarendon, Oxford **1982**.
[2] M. P. Allen, D. J. Tildesley, *Computer Simulation of Liquids*, Oxford University Press **1989**.
[3] P. Ungerer, C. Nieto Draghi, B. Rousseau, G. Ahunbay, V. Lachet, *J. Mol. Liq.* **2007**, *134*, 71 – 89.
[4] J. Vrabec, H. Hasse, *Mol. Phys.* **2002**, *100*, 3375 – 3383.
[5] C. Avendaño, T. Lafitte, C. S. Adjiman, A. Galindo, E. A. Müller, G. Jackson, *J. Phys. Chem. B* **2013**, *117*, 2717 – 2733.
[6] K. Stöbener, P. Klein, S. Reiser, M. Horsch, K.-H. Küfer, H. Hasse, *Fluid Phase Equilib.* **2014**, *373*, 100 – 108.
[7] B. Eckl, J. Vrabec, H. Hasse, *Fluid Phase Equilib.* **2008**, *274*, 16 – 26.
[8] E. N. Pistikopoulos, M. C. Georgiadis, V. Dua, C. S. Adjiman, A. Galindo, *Molecular Systems Engineering*, Wiley-VCH, Weinheim **2010**.
[9] C. W. Glass, S. Reiser, G. Rutkai, S. Deublein, A. Köster, G. Guevara Carrión, A. Wafai, M. Horsch, M. Bernreuther, T. Windmann, H. Hasse, J. Vrabec, *Comp. Phys. Comm.* **2014**, *185*, 3302 – 3306.
[10] H. Kahl, S. Enders, *Fluid Phase Equilib.* **2000**, *172*, 27 – 42.

[11] J. Groß, G. Sadowski, *Ind. Eng. Chem. Res.* **2001**, *40*, 1244 – 1260.
[12] P. Neumann, W. Eckhardt, H.-J. Bungartz, *Comput. Math. Appl.* **2014**, *67*, 272 – 281.
[13] C. Engin, H. M. Urbassek, *Nucl. Instrum. Meth.* **2013**, *295*, 72 – 75.
[14] D. W. Brenner, *Phys. Stat. Sol. B* **2000**, *217*, 23 – 40.
[15] E. H. Lee, J. Hsin, M. Sotomayor, G. Comellas, K. Schulten, *Structure* **2009**, *17*, 1295 – 1306.
[16] S. N. Wanasundara, R. J. Spiteri, R. K. Bowles, *J. Chem. Phys.* **2014**, 024505.
[17] S. Deublein, J. Vrabec, H. Hasse, *J. Chem. Phys.* **2012**, *136*, 084501.
[18] K. Langenbach, C. Engin, S. Reiser, M. Horsch, H. Hasse, *AIChE J.* **2015**, DOI:10.1002/aic.14820.
[19] G. Guevara Carrión, H. Hasse, J. Vrabec, *Top. Curr. Chem.* **2012**, *307*, 201 – 250.
[20] G. Guevara Carrión, J. Vrabec, H. Hasse, *Int. J. Thermophys.* **2012**, *33*, 449 – 468.
[21] S. Werth, K. Stöbener, P. Klein, K.-H. Küfer, M. Horsch, H. Hasse, *Chem. Eng. Sci.* **2015**, *121*, 110 – 117.
[22] Y.-L. Huang, J. Vrabec, H. Hasse, *Fluid Phase Equilib.* **2009**, *287*, 62 – 69.
[23] A. Heinecke, W. Eckhardt, M. Horsch, H.-J. Bungartz, *Supercomputing for Molecular Dynamics Simulations*, Springer, Heidelberg **2015**.
[24] G. Karniadakis, A. Beskok, N. Aluru, *Microflows and Nanoflows: Fundamentals and Simulation*, Springer, New York **2005**.
[25] H. Frentrup, C. Avendaño, M. Horsch, A. Salih, E. A. Müller, *Mol. Sim.* **2012**, *38*, 540 – 553.
[26] J. Kärger, D. M. Ruthven, D. N. Theodorou, *Diffusion in Nanoporous Materials*, Wiley-VCH, Weinheim **2012**.
[27] M. Horsch, J. Vrabec, *J. Chem. Phys.* **2009**, *131*, 184104.
[28] G. V. Lau, I. J. Ford, P. A. Hunt, E. A. Müller, G. Jackson, *J. Chem. Phys.* **2015**, *142*, 114701.
[29] S. Becker, H. M. Urbassek, M. Horsch, H. Hasse, *Langmuir* **2014**, *30*, 13606 – 13614.
[30] V. Kumar, S. Sridhar, J. D. Errington, *J. Chem. Phys.* **2011**, *135*, 184702.
[31] S. Kjelstrup, D. Bedeaux, E. Johannessen, J. Groß, *Non-Equilibrium Thermodynamics for Engineers*, World Scientific, Singapore **2010**.
[32] D. Wales, *Energy Landscapes: Applications to Clusters, Biomolecules and Glasses*, Cambridge University Press **2004**.
[33] P. L. Freddolino, C. B. Harrison, Y. Liu, K. Schulten, *Nature Phys.* **2010**, *6*, 751 – 758.

LIST OF FIGURES

Figure 1. *Saturated vapour and liquid densities for molecular models with one LJ site and two partial charges of equal magnitude and opposite sign, for different parameters and geometries of the molecular model [18]. The reduced dipole moment is varied between $\mu^* = 2$ (empty symbols) and 2.45 (full symbols), and the reduced distance between the two partial charges is $d^* = 0.3$ (▼), 0.4 (●), and 0.5 (▲), respectively. The LJ site is situated either at the same position as the negative partial charge (top) or in the middle between the two partial charges (bottom).*

Figure 2. *Left: Temperature dependence of the density (top) and the self-diffusion coefficient (bottom) of liquid ammonia at the pressure p = 10 MPa [20], from experiment (+) in comparison with an equation of state (—) as well as the molecular models by Feng et al. (∆) and Guevara et al. (○). Right: Dependence of the shear viscosity of liquid binary mixtures of ammonia and methanol on composition at constant pressure (p = 10 MPa) and temperature (T = 242, 298, and 373 K), cf. Guevara et al. [20], from a correlation of experimental data (—) in comparison with the molecular model by Guevara et al. (symbols).*

Figure 3. *Surface tension of real quadrupolar fluids from DIPPR correlations of experimental data (—) in comparison with predictions using molecular models of the 2CLJQ model class (□), cf. Werth et al. [21]. For the parameterization of the models, only bulk fluid properties were considered, whereas interfacial properties such as the surface tension were not taken into account.*

Figure 4. *Data structures for massively-parallel molecular simulations of systems with highly heterogeneous or fluctuating particle distributions, as implemented in the MD code ls1 mardyn [23]. The parallel processes are assigned different parts of the simulation volume (right). To simplify the neighbour search, the molecules are sorted into linked cells, and the size of the simulation volume corresponding to these cells is adapted to local density fluctuations (left).*

Figure 5. *Strong scaling, i.e. computing time required for a fixed-size simulation scenario over the number of parallel processes, in case of the MD simulation of a LJTS liquid droplet with N = 3 700 000 particles at the reduced temperature $T^* = 0.95$ using the ls1 mardyn program. For the volume-based domain decomposition, a subdivision into equal volumes (○) is compared with load balancing by recursive bisection employing a k-d tree data structure (■), cf. Fig. 4. The simulations were conducted on the hermit supercomputer at the High Performance Computing Center Stuttgart (HLRS).*

Figure 6. *Density profile of a LJTS liquid droplet with a reduced radius of $R^* = 15.8$ in a system containing N = 1 500 fluid particles at the reduced temperature $T^* = 0.8$ in contact with a planar solid surface with a reduced density of $\rho^* = 2.1$, also modelled by the LJTS potential, with a reduced fluid-solid interaction energy of $\zeta = 0.65$, cf. Becker et al. [29]. An approximation of the vapour-liquid interface by a sphere (—) yields a fluid-solid contact angle of $\theta = 60° \pm 2°$.*

Figure 7. *MD simulation of a planar vapour-liquid interface for a binary mixture of oxygen, represented by a 2CLJQ model, and carbon dioxide, represented by a 3CLJQ model, at T = 253 K and p = 6.5 MPa. Top: Visualization of a configuration, where each sphere corresponds to a LJ interaction size. Bottom: Partial density profile for both components, exhibiting an interfacial enrichment of oxygen at the interface.*

Figure 8. *Visualization of configurations from NEMD simulations of pressure-gradient driven Poiseuille flow of water through nanoporous carbon, represented here by a planar slit pore.*

Figure 1.

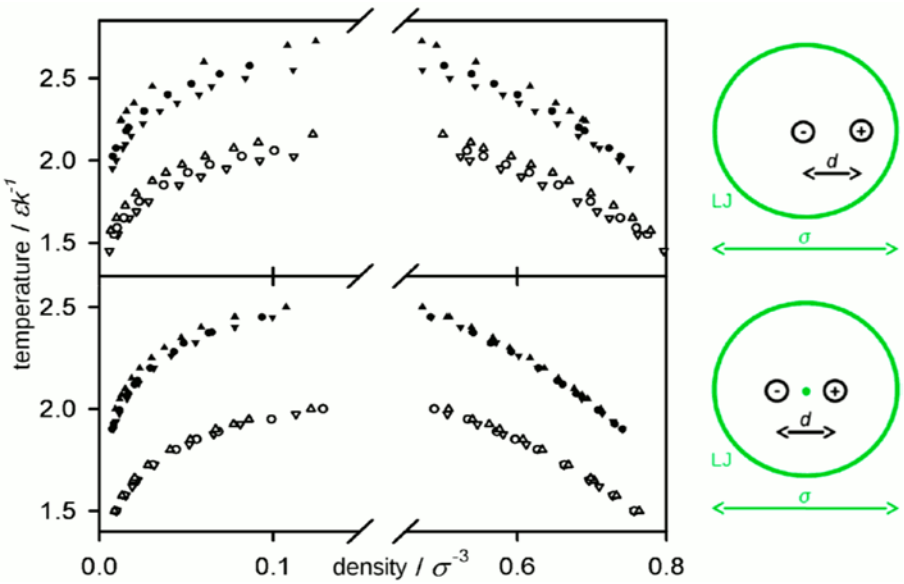
temperature / εk^{-1}
2.5
2.0
1.5
2.5
2.0
1.5
0.0
0.1
density / σ^{-3}
0.6
0.8
d
LJ
σ
d
LJ
σ

Figure 2.

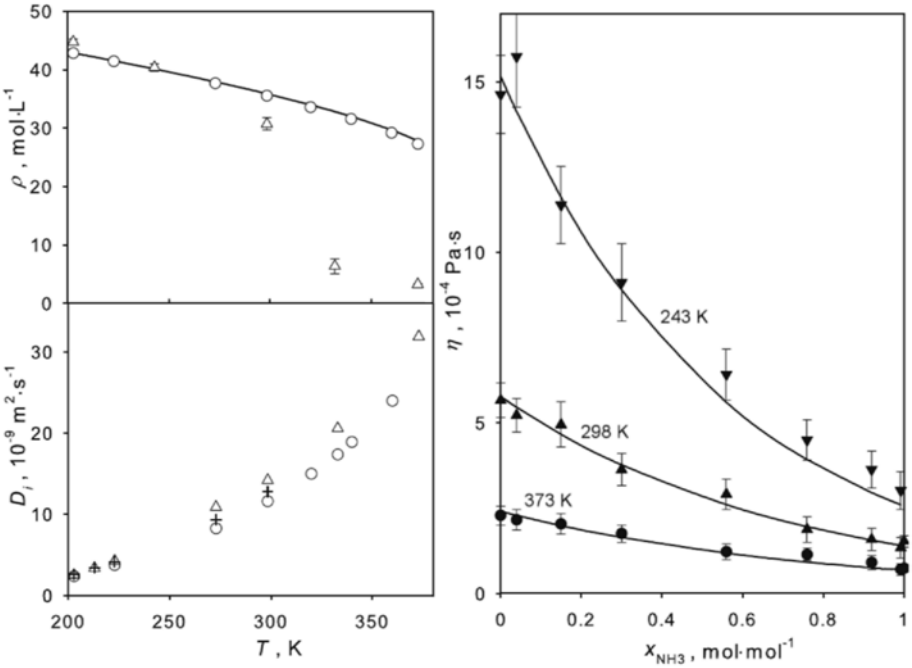

Figure 3.

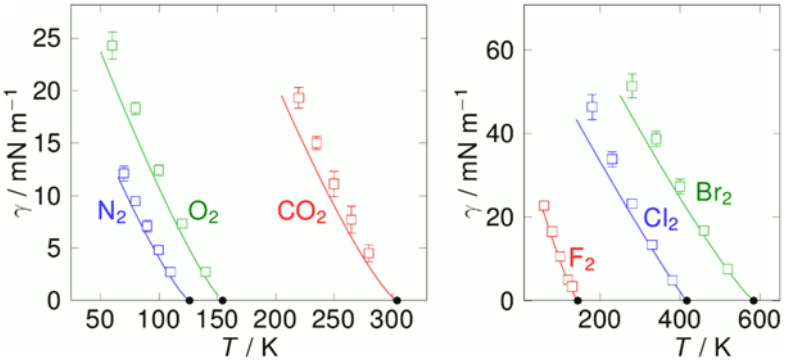
γ / mN m⁻¹
25
20
15
10
5
0
50
100
150
200
250
300
T / K
N2
O2
CO2
γ / mN m⁻¹
60
40
20
0
200
400
600
T / K
F2
Cl2
Br2

Figure 4.

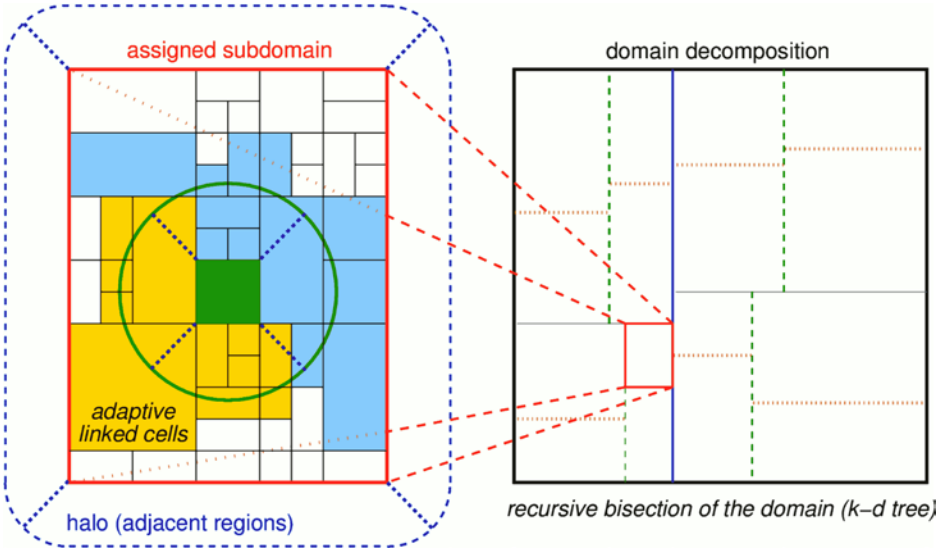
assigned subdomain
adaptive
linked cells
halo (adjacent regions)
domain decomposition
recursive bisection of the domain (k–d tree)

Figure 5.

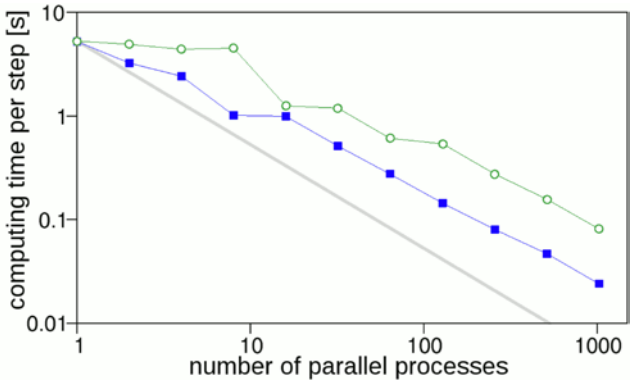
computing time per step [s]
10
1
0.1
0.01
1
10
100
1000
number of parallel processes

Figure 6.

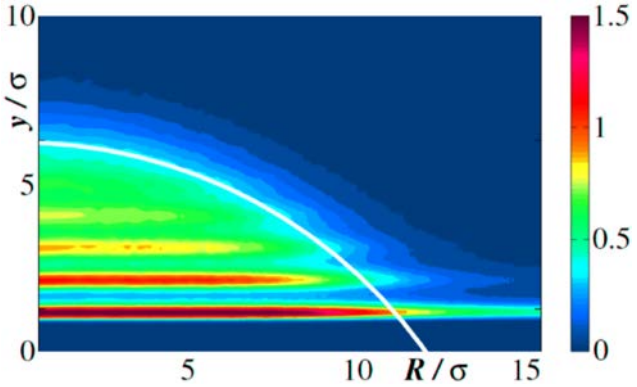

Figure 7.

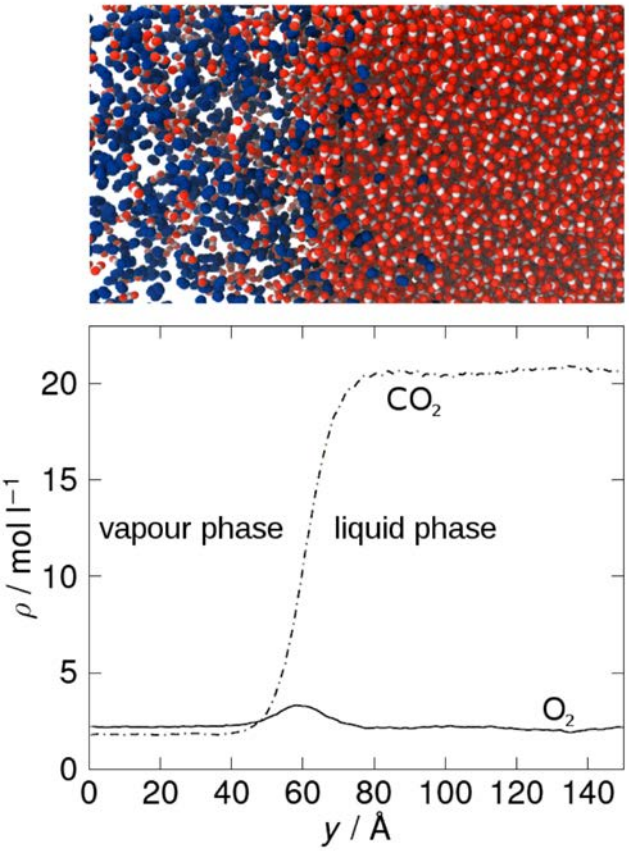
CO2
vapour phase
liquid phase
O2
ρ / mol l−1
y / Å
0
5
10
15
20
0
20
40
60
80
100
120
140

Figure 8.